SU(3) flavour breaking and baryon structure

A.N. Cooke[a], **R. Horsley**[a], **Y. Nakamura**[b], **D. Pleiter**[c,d], **P. E. L. Rakow**[e], **P. Shanahan**[f], **G. Schierholz**[g], **H. Stüben**[h], **J. M. Zanotti**[*,f]

[a] *School of Physics and Astronomy, University of Edinburgh, Edinburgh EH9 3JZ, UK*

[b] *RIKEN Advanced Institute for Computational Science, Kobe, Hyogo 650-0047, Japan*

[c] *JSC, Forschungszentrum Jülich, 52425 Jülich, Germany*

[d] *Institut für Theoretische Physik, Universität Regensburg, 93040 Regensburg, Germany*

[e] *Theoretical Physics Division, Department of Mathematical Sciences, University of Liverpool, Liverpool L69 3BX, UK*

[f] *CSSM, School of Chemistry and Physics, The University of Adelaide, Adelaide SA 5005, Australia*

[g] *Deutsches Elektronen-Synchrotron DESY, 22603 Hamburg, Germany*

[h] *Regionales Rechenzentrum, Universität Hamburg, 20146 Hamburg, Germany*

E-mail: james.zanotti@adelaide.edu.au

QCDSF/UKQCD Collaboration

We present results from the QCDSF/UKQCD collaboration for hyperon electromagnetic form factors and axial charges obtained from simulations using $N_f = 2+1$ flavours of $\mathcal{O}(a)$-improved Wilson fermions. We also consider matrix elements relevant for hyperon semileptonic decays. We find flavour-breaking effects in hyperon magnetic moments which are consistent with experiment, while our results for the connected quark spin content indicates that quarks contribute more to the spin of the Ξ baryon than they do to the proton.

---

[*]Speaker.

arXiv:1311.4916v1 [hep-lat] 19 Nov 2013

1. Introduction

It has long been known that the nucleon is not a point-like object, but in fact is composed of quarks and gluons. However, many questions still remain, such as how are these constituents distributed inside the nucleon? And how do they combine to produce its experimentally observed properties? For example, experimental results revealed that the quark spin contribution to the spin of the proton is only about 30%. This was originally termed the "spin crisis", however this quickly became more of a "spin puzzle" as it was observed that quark orbital angular momentum and gluon angular momentum would also contribute to the total spin of the proton, although the exact decomposition remains unclear. Given this observed suppression of the quark spin content of the proton, an interesting quesion to ask is whether or not this is a property unique to the nucleon, or a univeral feature of all hadrons.

Hence understanding how the nucleon and other hadrons are constructed from their quark and gluon constituents remains one of the most important and challenging questions in modern nuclear physics. The study of the electromagnetic (EM) properties of hadrons, to cite another example, provides important insights into the non-perturbative structure of QCD. The EM form factors reveal information on the internal structure of hadrons including their size, charge distribution and magnetisation. While only a few hyperon properties have been determined experimentally (e.g. for the electric charge radii, only p, n, Σ^- have been measured), on the lattice they should (in principle) be easier to calculate than nucleon observables due to the presence of the heavier strange quark.

Lattice simulations have the potential to provide insights into the charge and magnetic distribution of hyperons as well as the role of SU(3)-flavour symmetry breaking in these distributions, which experiment cannot currently provide. These are of significant interest as they provide valuable insights into the environmental sensitivity of the distribution of quarks inside a hadron. For example, how does the distribution of u quarks in Σ^+ change as we change the mass of the (spectator) s quark? Simulations can also provide insights into the role of hidden flavour (e.g. strangeness in the proton) [1, 2]. However, while the EM form factors of the nucleon have received a lot of recent attention in lattice simulations (see, e.g., [3] for a review), the investigation of the hyperon EM form factors has so far received only limited attention [4, 5].

Lattice simulations are currently performed in the isospin-symmetric limit ($m_u = m_d$) (see [6] for recent progress in isospin-breaking effects). However, QCD is flavour-blind, so we could think of the s quark as a very heavy d quark and compare lattice results for $\Sigma^+(uus)$ with the proton (uud) to gain an idea of the implications for isospin-breaking. This idea has already been explored in the context of the first lattice determinations of charge-symmetry violation in moments of spin-independent [7] and spin-dependent [8] parton distribution functions.

Semileptonic form factors of the hyperons provide an alternative method to the standard $K_{\ell 3}$ decays (see e.g. [9]) for determining the CKM matrix element, $|V_{us}|$. Earlier quenched and $N_f = 2$ results for $\Sigma^- \to n\ell\nu$ and $\Xi^0 \to \Sigma^+\ell\nu$ can be found in [10, 11], while more recent $N_f = 2 + 1$ results have been obtained in [12].

In this talk we present preliminary results from the QCDSF/UKQCD Collaboration for the octet hyperon electromagnetic and semileptonic decay form factors, as well as their axial charges, determined from $N_f = 2 + 1$ lattice QCD.

	κ_l	κ_s	$V = L^3 \times T$	m_π [MeV]	m_K [MeV]	$m_\pi L$
1	0.120900	0.120900	$32^3 \times 64$	440	440	5.6
2	0.121040	0.120620	$32^3 \times 64$	340	480	4.3
3	0.121095	0.120512	$32^3 \times 64$	290	490	3.7
4	0.121166	0.120371	$48^3 \times 96$	220	520	4.1

Table 1: Simulation details for the subset of ensembles used here with $a = 0.078(3)$ fm [15].

2. Simulation Details

Our gauge field configurations have been generated with $N_f = 2 + 1$ flavours of dynamical fermions, using the tree-level Symanzik improved gluon action and nonperturbatively $\mathscr{O}(a)$ improved Wilson fermions [13]. We choose our quark masses by first finding the $SU(3)_{\text{flavour}}$-symmetric point where flavour singlet quantities take on their physical values, then varying the individual quark masses while keeping the singlet quark mass $\overline{m}_q = (m_u + m_d + m_s)/3 = (2m_l + m_s)/3$ constant [14]. We have generated a large set of ensembles of varying quark masses and volumes at $\beta = 5.50$, corresponding to a lattice spacing, $a = 0.078(3)$ fm, where we have used the average baryon octet mass, X_N, to set the scale [15]. We are now in the process of generating configurations at additional lattice spacings to enable the continuum limit to be taken. The results presented in this proceedings are obtained on a subset of the complete set of ensembles. A summary of the parameter space spanned by our dynamical configurations can be found in Table 1. More details regarding the tuning of our simulation parameters are given in Refs. [14, 15].

In this preliminary work, we will not study systematic errors such as potential contributions of disconnected diagrams, excited state contamination or discretisation effects. However, we hope that these effects are likely to be similar for different members of the baryon octet and so perhaps are not relevant for our investigation of SU(3)-breaking effects.

3. Electromagnetic Form Factors

On the lattice, we determine the form factors $F_1(q^2)$ and $F_2(q^2)$ by calculating the following matrix element of the electromagnetic current

$$\langle B(p', s')|j_\mu(q)|B(p, s)\rangle = \bar{u}(p', s')\left[\gamma_\mu F_1(q^2) + \sigma_{\mu\nu}\frac{q_\nu}{2M_B}F_2(q^2)\right]u(p, s), \qquad (3.1)$$

where $u(p, s)$ is a Dirac spinor with momentum p, and spin polarisation s, $q = p' - p$ is the momentum transfer, M_B is the mass of the baryon B, and j_μ is the electromagnetic current. The Dirac (F_1) and Pauli (F_2) form factors of the proton are obtained by using $j_\mu^{(p)} = \frac{2}{3}\bar{u}\gamma_\mu u - \frac{1}{3}\bar{d}\gamma_\mu d$, while the form factors for the Σ and Ξ baryons are obtained through the appropriate substitution, $u \to s$ or $d \to s$. It is common to rewrite the form factors F_1 and F_2 in terms of the electric and magnetic Sachs form factors, $G_e = F_1 + q^2/(2M_N)^2 F_2$ and $G_m = F_1 + F_2$.

If one is using a conserved current, then (e.g. for the proton) $F_1^{(p)}(0) = G_e^{(p)}(0) = 1$ gives the electric charge, while $G_m^{(p)}(0) = \mu^{(p)} = 1 + \kappa^{(p)}$ gives the magnetic moment, where $F_2^{(p)}(0) = \kappa^{(p)}$ is the anomalous magnetic moment. From Eq. (3.1) we see that F_2 always appears with a factor
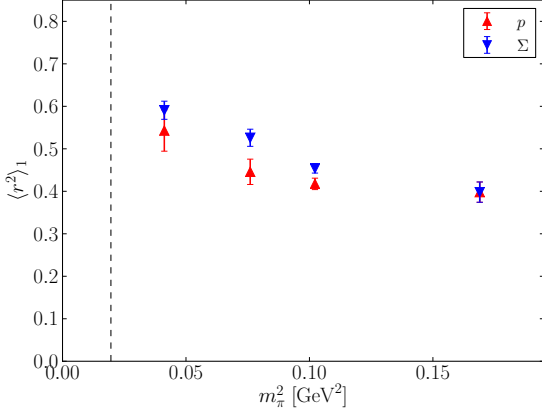
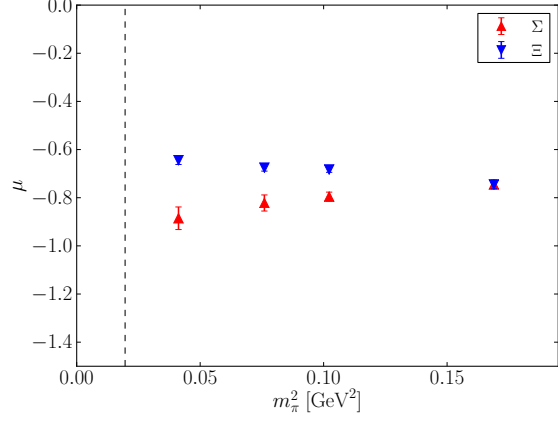**Figure 1:** Dirac charge radii for the proton and Σ^+. Vertical dashed line represents the physical point.

Figure 2: Magnetic moments for the Σ^- and Ξ^-. Vertical dashed line represents the physical point.

of q, so it is not possible to extract a value for F_2 at $q^2 = 0$ directly from our lattice simulations. Hence we are required to extrapolate the results we obtain at finite q^2 to $q^2 = 0$.

We perform dipole fits $F(q^2) = F(0)/(1 - q^2/M^2)^2$ to F_1 and F_2, although it was found in [16] that $F_1(q^2)$ and $F_2(q^2)$ are better described by the ansätze $F_1(q^2) = F_1(0)/(1 + c_{12}q^2 + c_{14}q^4)$, and $F_2(q^2) = F_2(0)/(1 + c_{12}q^2 + c_{16}q^6)$. This will be explored in future work.

Form factor radii, $r_i = \sqrt{\langle r^2 \rangle_i}$, are defined from the slope of the form factor at $q^2 = 0$. In this talk, we are primarily interested in searching for any $SU(3)$-flavour breaking effects in the octet hyperon form factors. Fig. 1 shows the Dirac radii, $\langle r^2 \rangle_1$, of the proton and Σ^+. This example is interesting as they are both charge $+1$, contain 2 up quarks, and one charge $-1/3$ quark. In the case of the proton this singly-represented quark is a light down quark, while in the Σ^+ it is a heavier strange quark. Starting from the SU(3)-symmetric limit where the p and Σ are degenerate and hence have the same charge radius, we see similar quark mass behaviour, but interestingly, we find the charge radius of the Σ^+ to be slightly larger than that of the proton.

Fig. 2 shows the magnetic moments of the Σ^- and Ξ^- hyperons. These baryons are both charge -1, and contain three charge $-1/3$ quarks. In the case of the Σ^- this is 2 light and one strange, while in the Ξ^- this is reversed. In the plot we see that the baryons have degenerate magnetic moments in the SU(3)-flavour limit, but as we change the quark masses and approach the physical point, denoted by the vertical dashed line, we observe a definite splitting between the two magnetic moments, with the ordering in agreement with experiment.

4. Hyperon Axial Charges

Hyperon axial charges are important for a low-energy effective field theory description of octet baryons. In the SU(3)-flavour limit, the hyperon axial charges are described by two low energy constants, F and D, e.g.

$$g_A^{NN} = F + D, \; g_A^{\Sigma\Sigma} = F, \; g_A^{\Xi\Xi} = F - D, \; g_A^{\Xi\Xi} = F + D \,, \tag{4.1}$$

where in our notation, the initial and final baryon states are given as a superscript, so the standard nucleon axial charge is denoted, g_A^{NN}, while the axial charge relevant to the $\Xi \to \Sigma$ semileptonic

4

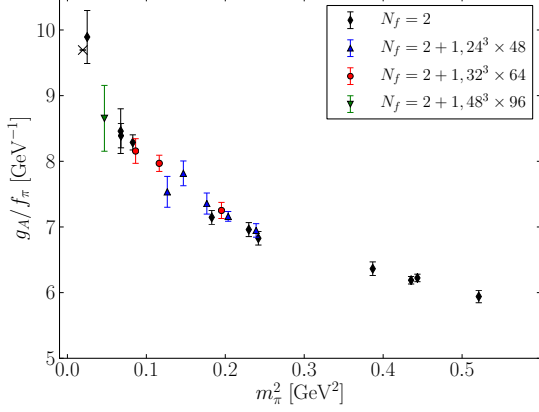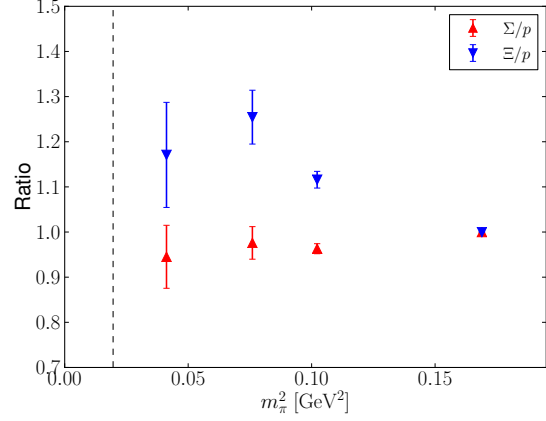**Figure 3:** $N_f = 2 + 1$ results for g_A/f_π compared with $N_f = 2$ results from [21].

Figure 4: Ratio of the quark spin content of the Σ and Ξ to that of the proton.

decay (see next section) is denoted, $g_A^{\Xi\Sigma}$. The F and D constants, which describe all hyperon axial charges, enter the chiral expansion of every baryonic quantity, e.g. masses. Despite this, they are poorly determined. Quark models, chiral perturbation theory, large-N_c and fits to hyperon beta decay give a range of results [17, 18, 19], $F \approx 0.3 - 0.5$, $D \approx 0.6 - 0.8$. Since we are interested in SU(3)-flavour breaking effects, we will be looking for deviations from the expressions in Eq. (4.1). We have recently worked out the SU(3)-flavour breaking effects in baryon matrix elements up to NLO [20] which can be used to fit lattice results once a sufficient collection of axial charges is available. Here we will investigate only a couple of axial charges.

The first quantity we will consider is the ratio g_A/f_π, as proposed in [21], as it is naturally renormalised and has reduced finite size and discretisation effects. In Fig. 3 we compare our $N_f = 2 + 1$ results from the current work with the $N_f = 2$ results from [21] and we find excellent agreement, with a smooth trend towards the physical point.

It is long known that intrinsic quark spin contributes only about 33% of the total spin of the proton. In Fig. 4 we look for signs of similar spin suppression in other hyperons by considering the ratio of the total connected quark contribution to the Σ and Ξ spins to that of the proton. This idea was first proposed in [22] using some of our earlier results from [8]. Our new results exhibit similar findings, namely that the total connected quark spin contribution in the Σ is similar to that of the proton, while a larger fraction of the Ξ baryon spin comes from the quark spin. Hence this is a clear indication that quark spin suppression in hadrons is not universal.

5. Hyperon Semileptonic Form Factors

Semileptonic form factors of the hyperons provide an alternative method for determining the CKM matrix element, $|V_{us}|$. This is done by using the experimental value for the decay rate of the hyperon beta decays, $B \to b\ell\nu$, to obtain the combination

$$|V_{us}|^2 |f_1(0)|^2 \left(1 + 3 \left| \frac{g_1(0)}{f_1(0)} \right|^2 \right) . \tag{5.1}$$

Hence for a determination of $|V_{us}|$, we need to know the vector and axial form factors, $f_1(q^2)$ and $g_1(q^2)$, at zero momentum transfer ($q^2 = 0$).
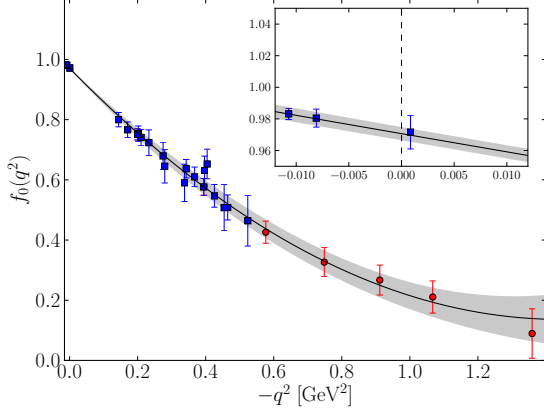
Figure 5: $f_0(q^2)$ for the $\Sigma^- \to n\ell\nu_\ell$ decay from a $32^3 \times 64$ lattice with $m_\pi \approx 340$ MeV.
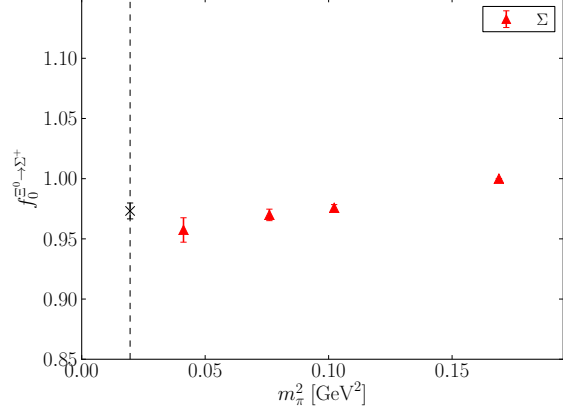
Figure 6: Quark mass dependence of $f_0(0) = f_1(0)$ for the $\Xi^0 \to \Sigma^+\ell\nu_\ell$ decay.

The vector and axial matrix elements for $SU(3)$-octet baryon semileptonic decays are each given in terms of 3 form factors: vector (f_1), weak magnetism (f_2), induced scalar (f_3), axial-vector (g_1), weak electricity (g_2) and induced pseudoscalar (g_3) (see e.g. [11]). For a lattice calculation of hyperon beta decays, it is useful to define the scalar form factor $f_0(q^2) = f_1(q^2) + \frac{q^2}{M_B^2 + M_b^2} f_3(q^2)$, which can be obtained at $q^2_{\max} = (M_B - M_b)^2$ with high precision [23]. Interpolating lattice results obtained at finite q^2 values to $q^2 = 0$ leads to the desired result $f_0(0) = f_1(0)$. To reduce the systematic error involved in this q^2 interpolation, it has been shown that twisted boundary conditions greatly help in the context of $K_{\ell 3}$ decays [24, 25]. For some of our ensembles, we have implemented this technique for hyperon semileptonic decays in order to assess their effectiveness.

In Fig. 5 we present some results for $f_0(q^2)$ for the $\Sigma^- \to n\ell\nu_\ell$ decay from a $32^3 \times 64$ lattice with $m_\pi \approx 340$ MeV. The red circles indicate results obtained using only Fourier momenta, while results obtained using twisted boundary conditions are given by blue squares. We zoom into the region of interest around $q^2 = 0$ in the insert, where we see that our choice of twists enable us to obtain a result directly at $q^2 = 0$.

After interpolating $f_0(q^2)$ to $q^2 = 0$, we investigate the quark mass dependence of $f_0(0)$ in Fig. 6 and compare our result to the extrapolated result from [12]. Although we haven't yet performed our chiral extrapolation, we will complete this soon in the context of SU(3)-flavour breaking expansions [20].

Acknowledgements

References

[1]   D. B. Leinweber *et al.*, Phys. Rev. Lett. **94** (2005) 212001 [hep-lat/0406002].

[2]   D. B. Leinweber *et al.*, Phys. Rev. Lett. **97** (2006) 022001 [hep-lat/0601025].

[3]   Ph. Hägler, Phys. Rept. **490** (2010) 49 [0912.5483 [hep-lat]].

[4]   S. Boinepalli *et al.*, Phys. Rev. **D74** (2006) 093005 [hep-lat/0604022].

[5]   H. -W. Lin and K. Orginos, Phys. Rev. **D79** (2009) 074507 [0812.4456 [hep-lat]].

[6]   N. Tantalo, PoS LATTICE **2013** (2013) 007 [1311.2797 [hep-lat]].

[7]   R. Horsley *et al.*, Phys. Rev. D **83** (2011) 051501 [1012.0215 [hep-lat]].

[8]   I. C. Cloet *et al.*, Phys. Lett. B **714** (2012) 97 [1204.3492 [hep-lat]].

[9]   N. Cabibbo, E. C. Swallow and R. Winston, Ann. Rev. Nucl. Part. Sci. **53** (2003) 39 [hep-ph/0307298].

[10] D. Guadagnoli *et al.*, Nucl. Phys. B **761** (2007) 63 [hep-ph/0606181].

[11] S. Sasaki and T. Yamazaki, Phys. Rev. **D79** (2009) 074508 [0811.1406 [hep-ph]].

[12] S. Sasaki, Phys. Rev. D **86** (2012) 114502 [1209.6115 [hep-lat]].

[13] N. Cundy *et al.* [QCDSF/UKQCD Collaboration], Phys. Rev. **D79** (2009) 094507 [0901.3302 [hep-lat]].

[14] W. Bietenholz *et al.* [QCDSF/UKQCD Collaboration], Phys. Lett. **B690** (2010) 436 [1003.1114 [hep-lat]].

[15] W. Bietenholz *et al.* [QCDSF/UKQCD Collaboration], Phys. Rev. D **84** (2011) 054509 [1102.5300 [hep-lat]].

[16] S. Collins *et al.* [QCDSF Collaboration], Phys. Rev. D **84** (2011) 074507 [1106.3580 [hep-lat]].

[17] K. -S. Choi, W. Plessas and R. F. Wagenbrunn, Phys. Rev. D **82** (2010) 014007 [1005.0337 [hep-ph]].

[18] F. E. Close and R. G. Roberts, Phys. Lett. B **316** (1993) 165 [hep-ph/9306289].

[19] J. M. Gaillard and G. Sauvage, Ann. Rev. Nucl. Part. Sci. **34** (1984) 351.

[20] A. N. Cooke *et al.* [QCDSF Collaboration], PoS LATTICE **2012** (2012) 116 [1212.2564 [hep-lat]].

[21] R. Horsley *et al.* [QCDSF/UKQCD Collaboration], 1302.2233 [hep-lat].

[22] P. E. Shanahan *et al.*, Phys. Rev. Lett. **110** (2013) 202001 [1302.6300 [nucl-th]].

[23] S. Hashimoto *et al.*, Phys. Rev. **D61** (1999) 014502 [hep-ph/9906376].

[24] P. A. Boyle *et al.* [RBC/UKQCD Collaboration], Eur. Phys. J. C **69** (2010) 159 [1004.0886 [hep-lat]].

[25] P. A. Boyle *et al.* [RBC/UKQCD Collaboration], JHEP **1308** (2013) 132 [1305.7217 [hep-lat]].

[26] Y. Nakamura and H. Stüben, PoS LATTICE **2010** (2010) 040 [1011.0199 [hep-lat]].

[27] P. A. Boyle, Comp. Phys. Comm. **180**, (2009) 2739.

[28] R. G. Edwards and B. Joó, Nucl. Phys. Proc. Suppl. **140** (2005) 832 [hep-lat/0409003].